Supplementary Materials

Limits of Directed Self-Assembly in Block Copolymers

K. R. Gadelrab[1], Yi Ding[1], Ricardo Pablo-Pedro[2], Hsieh Chen[1], Kevin W. Gotrik[1], David G. Tempel[1], Caroline A. Ross[1], and Alfredo Alexander-Katz*[1]

[1]Department of Material Science and Engineering, Massachusetts Institute of Technology, Cambridge, Massachusetts 02139, USA.

[2]Department of Chemistry, Massachusetts Institute of Technology, Cambridge, Massachusetts 02139, USA

**E-mail: aalexand@mit.edu*

Experimental Methods

Post fabrication: In a typical experiment, the template of posts was fabricated by spin-coating 4% hydrogen silsesquioxane (HSQ) onto a Si substrate to a thickness of 42nm before subsequently exposed by electron beam lithography (EBL, Elionix ELS-F125) at an acceleration voltage of 125kV and current of 1nA. The dosage was kept at 120fC. The exposed HSQ thin film was subsequently developed in 4 wt% NaOH and 1 wt% NaOH aqueous solution for 4min, followed by rinsing with de-ionized water (2min) and isopropanol (10s). The samples were then dried by N_2.

Brush grafting: Hydroxyl-terminated polydimethylsiloxane (PDMS) brush (0.8kg mol^{-1}, 1% in a solvent of propylene glycol methyl ether acetate, PGMEA) was covalently bonded to the surface of both the posts and the substrate by spin-coating at 3k rpm and baking at 140^{o}C in a vacuum oven (~20torr) for 18h. After being taken out of the oven, the samples were rinsed with toluene for 30s to remove the unreacted PDMS molecules.

Spin-coating and annealing: The block copolymer polystyrene-block-polydimethylsiloxane (PS-*b*-PDMS) (minority volume fraction f_{PDMS} = 16.5%, molecular weight 51.5 kg/mol, PDI = 1.04, 1 wt% in PGMEA) was subsequently spin-coated to a thickness of 38nm.The sample was annealed in a chamber of a mixed solvent of toluene and -heptane (5:1 in volume ratio) for 30s at room temperature, followed by a thermal quenching at 60^{o}C for 5s (K. Gotrik et al., ***Nano Lett.***, 2013, 13 5117). The samples were then removed in a few sec from the annealing chamber.

Plasma etching: After annealing, a reactive-ion etching process of 5s CF_4 (50W, 15 mTorr) followed by 22s of O_2 (90W, 6mTorr) was used to remove the surface coating PDMS layer and the PS matrix, and to subsequently oxidize the PDMS block into amorphous silica.

SEM images were taken by using an Elionix ELS-F125 electron microscope at 125kV.

To create the coordinates of each post for ‹11›and ‹20› phases on a hexagonal lattice with period L_0 at different levels of noise, a computer program was written in Mathematica. We first generated the perfect coordinates for the

‹11›and ‹20› phases followed by adding a random normal Gaussian distribution with mean zero and a variance $\zeta^2 L_0^2$. In figure S1, the distribution of noise around a post is shown where ζ is the variance or magnitude of noise which is randomly distributed over [0, 2π]. Then, the templates were fabricated with the coordinates obtained from the computer program using electron beam patterning of HSQ.

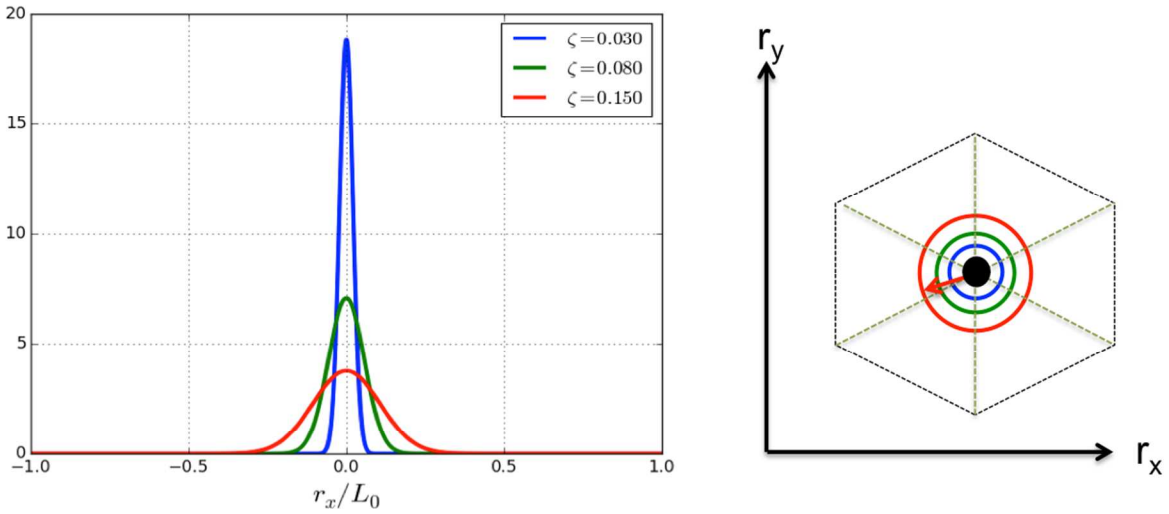

Fig. S1. **1D probability distribution of a post (black dot) at different levels of noise. The coordinate of the post is (0,0).**

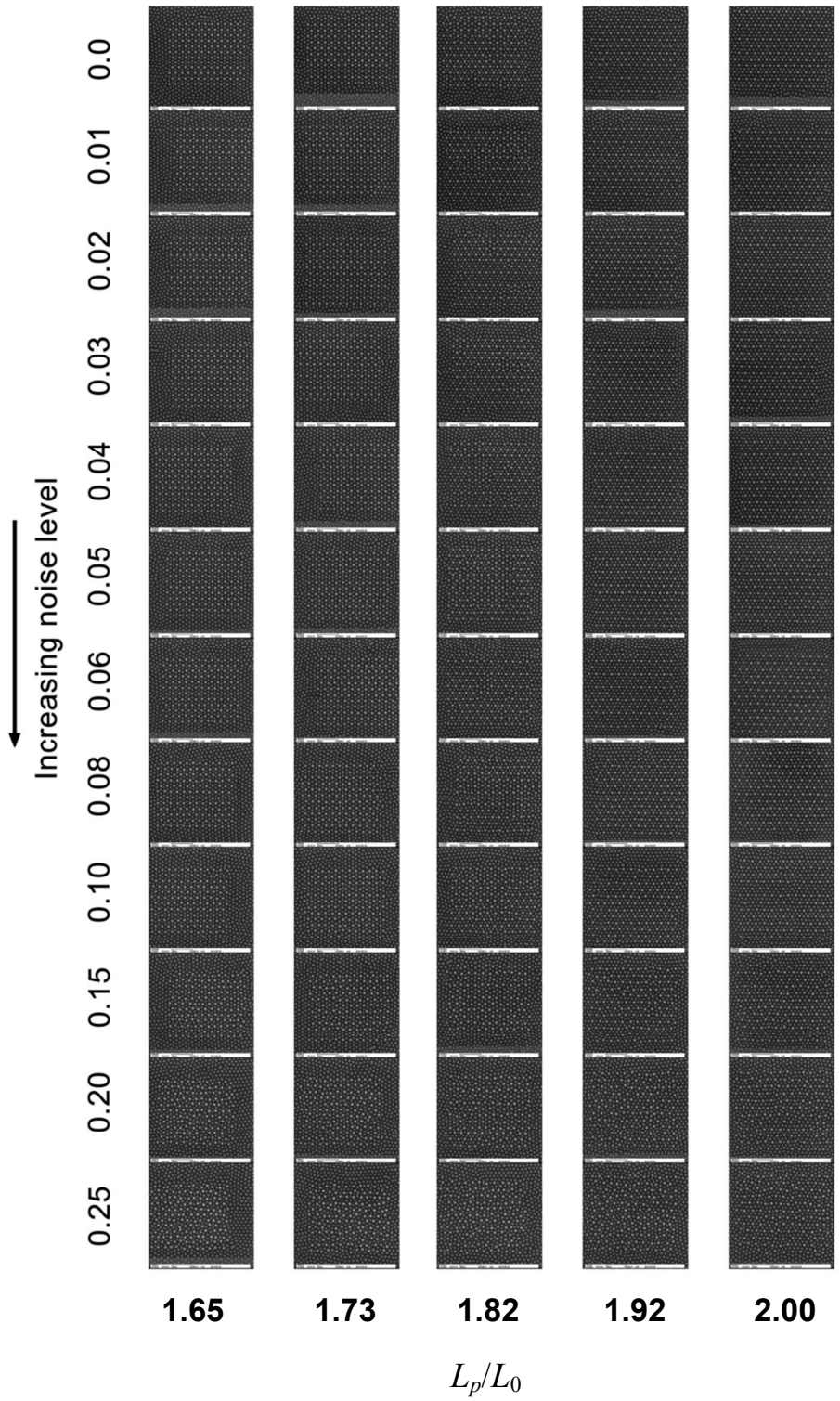

Fig. S2. Experimental data for templated post patterns with different amounts of noise and different post spacings.

Post correlation Orientational correlation function

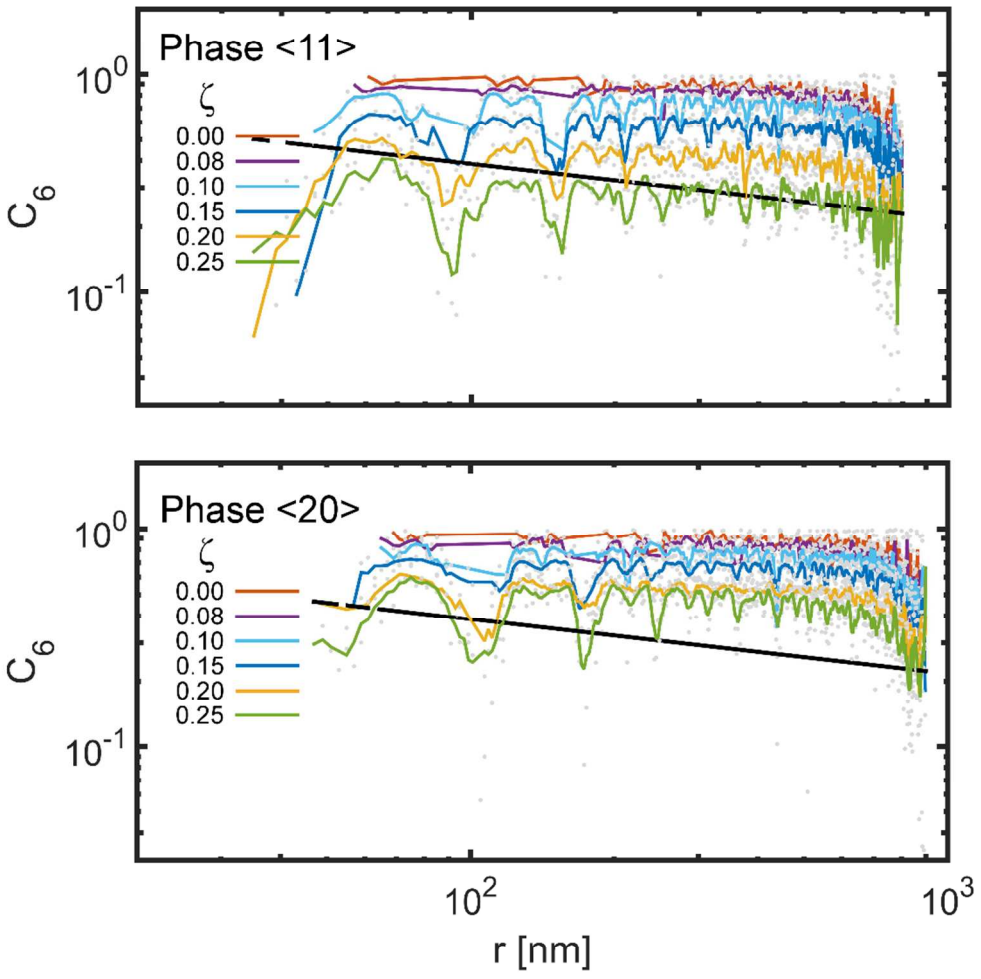

Fig.S3. **Orientation correlation function C_6 for the experimental results for only the *post pattern* of both the ‹11›, and ‹20› phases at different noise levels. The hexatic-liquid transition at a slope of $\eta_6 = ¼$ is marked in dash line.**

Experimental Orientational correlation functions for set 2

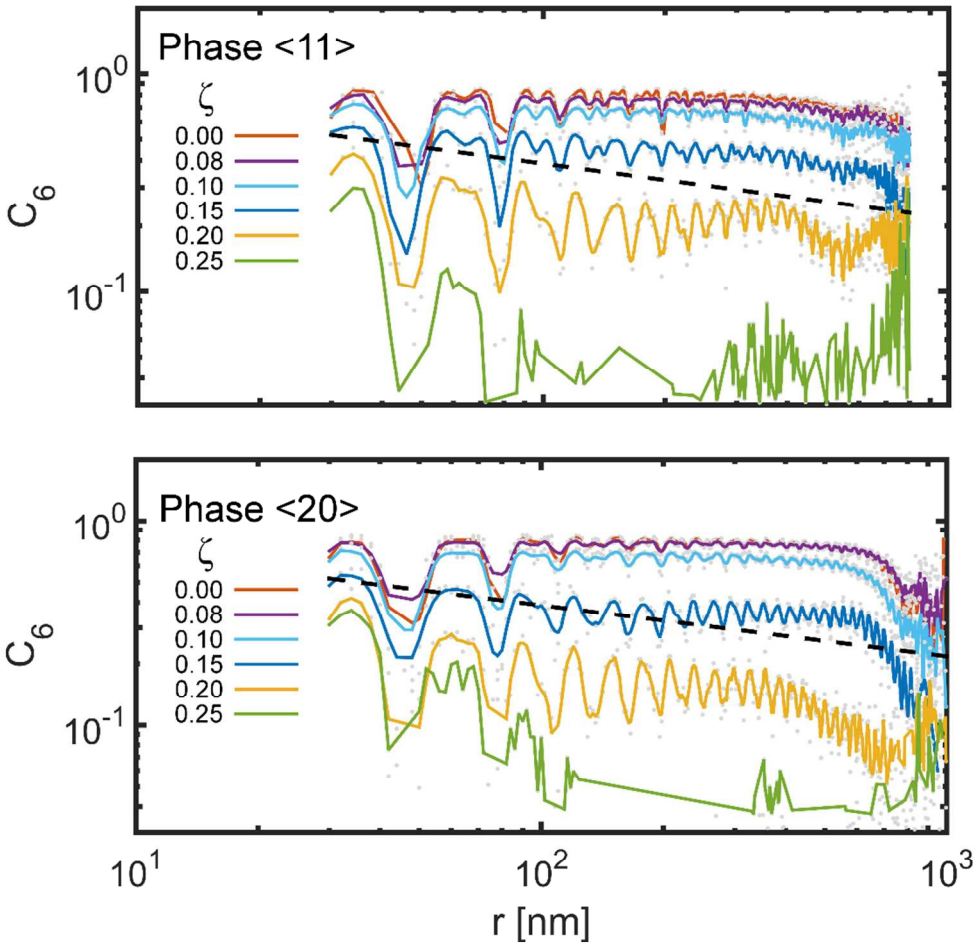

Fig.S4. **Orientation correlation function C_6 for the experimental results of *set 2* of both ‹11›, and ‹20› phases at different noise levels. The hexatic-liquid transition at a slope of η_6 = ¼ is marked by a dashed line. The behavior of C_6 of this independent dataset matches the results in the main text of figure 3.**

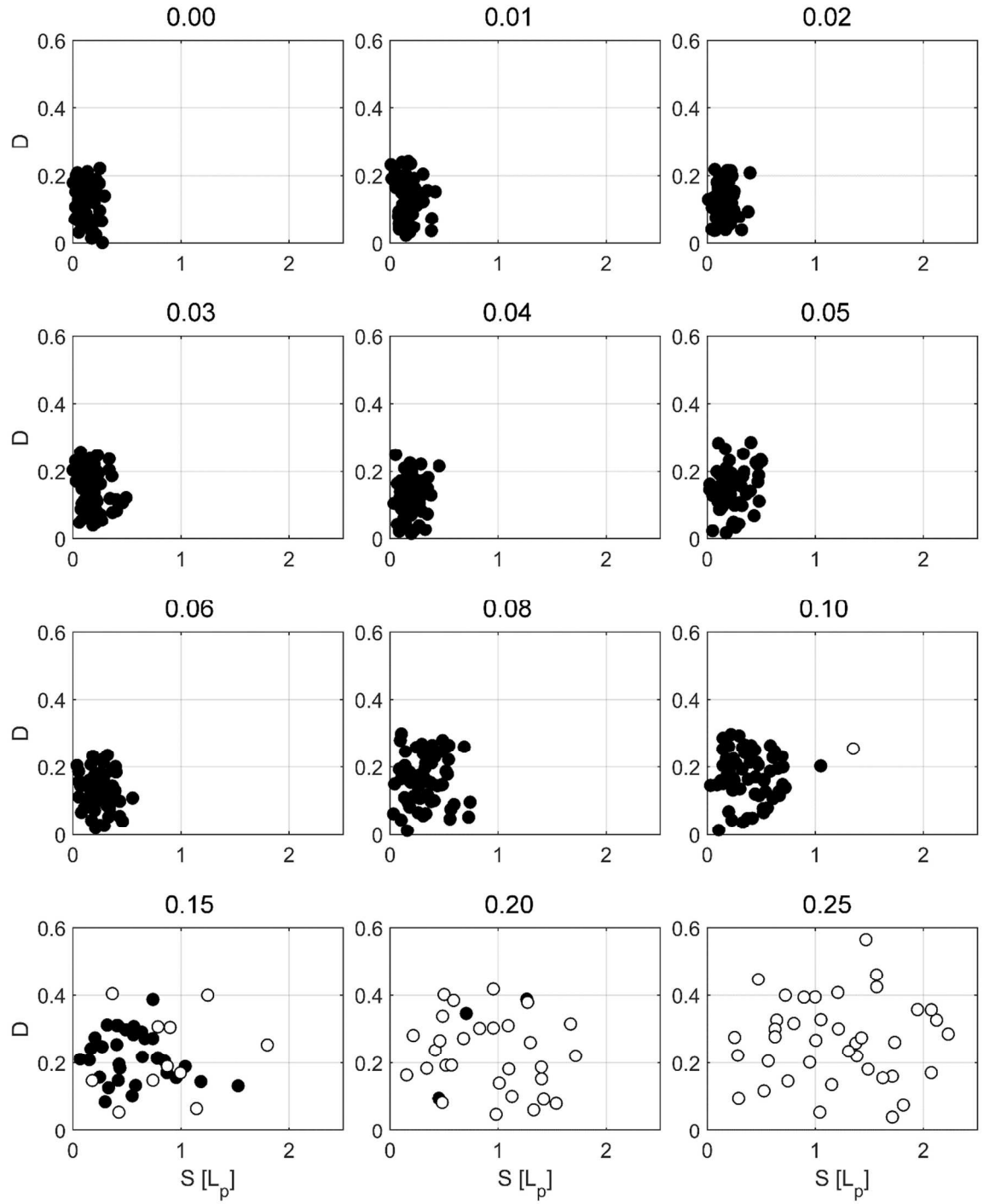

Fig.S5. **Distortion *S* and dilation *D* parameters for different template hexagons for the complete noise level range (shown on each plot) for the ‹11› phase of set-1. Sample of the data is shown in figure 4a. Unfilled markers represent template hexagons with defects (center post or a polymer domain in its vicinity not coordinated by 6 nearest neighbors).**

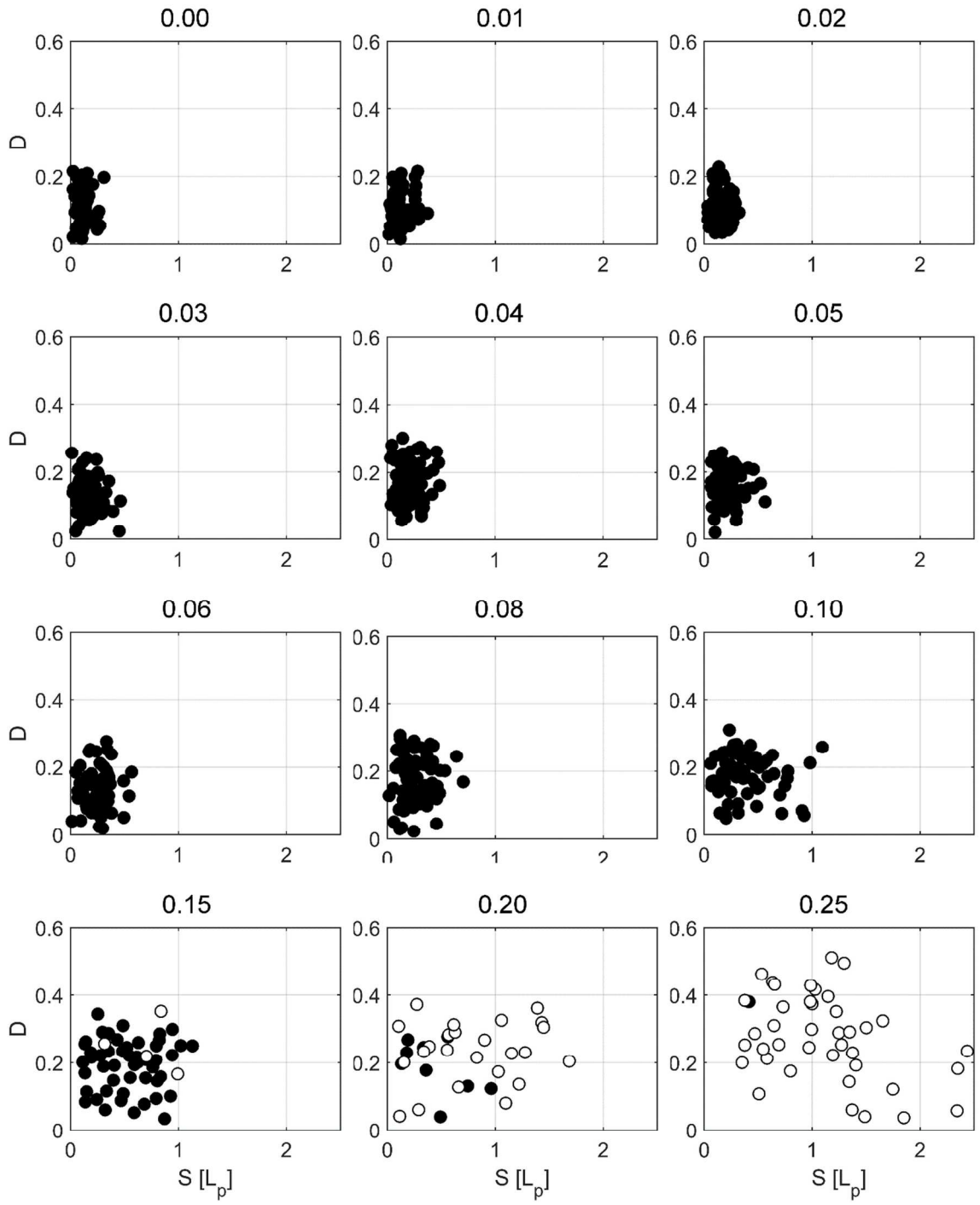

Fig.S6. **Distortion *S* and dilation *D* parameters for different template hexagons for the complete noise level range (shown on each plot) for the ‹11› phase of set-2. Unfilled markers represent template hexagons with defects (center post or a polymer domain in its vicinity not coordinated by 6 nearest neighbors).**

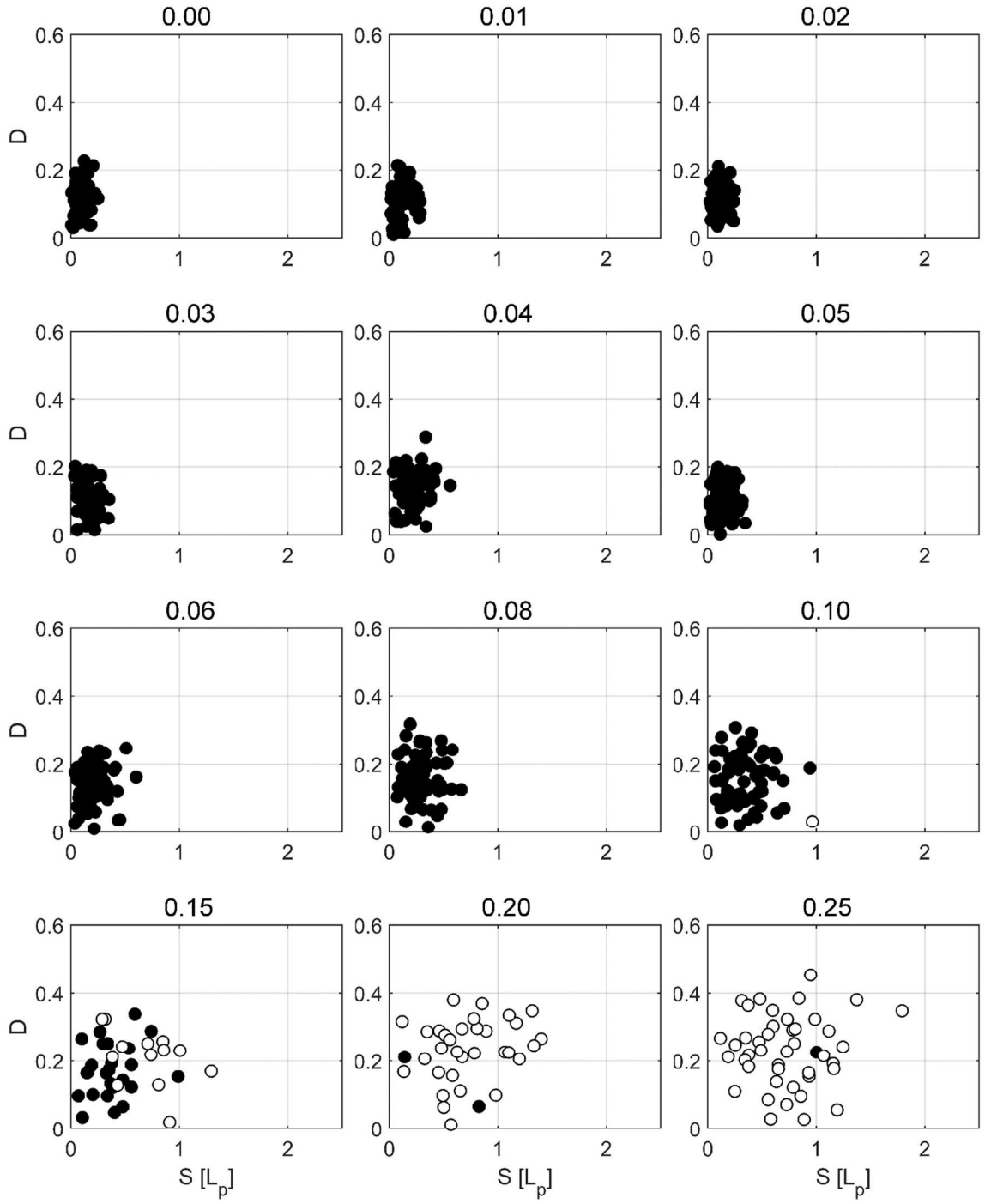

Fig.S7. **Distortion *S* and dilation *D* parameters for different template hexagons for the complete noise level range (shown on each plot) for the ‹20› phase of set-1. Sample of the data is shown in figure 4b. Unfilled markers represent template hexagons with defects (center post or a polymer domain in its vicinity not coordinated by 6 nearest neighbors).**

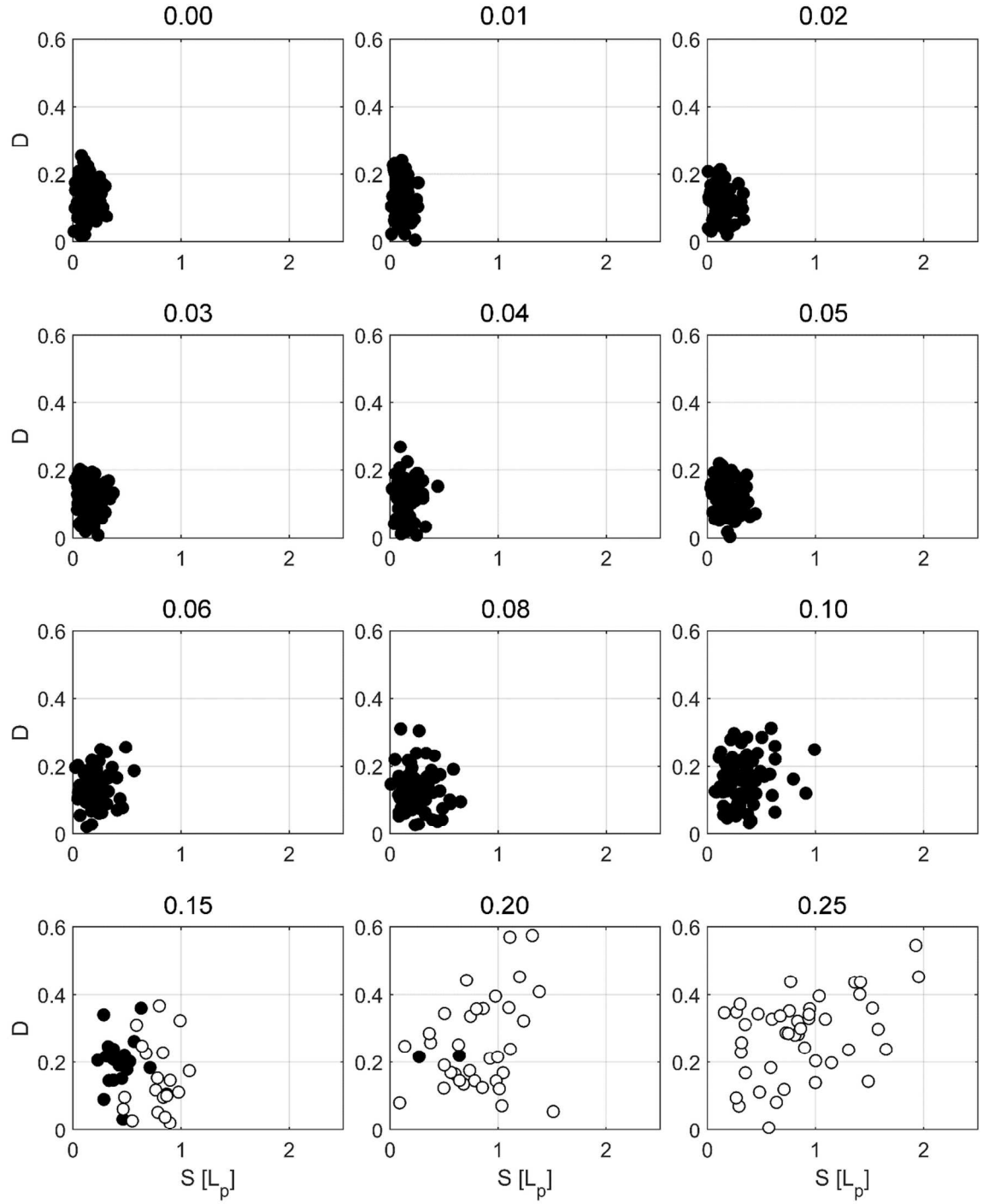

Fig.S8. **Distortion *S* and dilation *D* parameters for different template hexagons for the complete noise level range (shown on each plot) for the ‹20› phase of set-2. Unfilled markers represent template hexagons with defects (center post or a polymer domain in its vicinity not coordinated by 6 nearest neighbors).**

Simulations:

Self-consistent field theory (SCFT) simulations have been shown to faithfully capture the equilibrium structures of block copolymers and agree very well with experiments. Here, we briefly describe the formalism of SCFT simulations of diblock copolymers.

We consider a monodispersed melt of n A-B diblock copolymer of volume V, with each diblock molecule is composed of N segments. The A and B blocks consists of fN and $(1-f)N$ chain segments, respectively. The interaction between the dissimilar blocks is controlled by a Flory-Huggins parameter χ. Within the mean-field approximation, the free energy of the system F is expressed in terms of field variables

$$\frac{F}{nk_BT} = \frac{1}{V}\int d\vec{r}\left(\chi N\phi_A(\vec{r})\phi_B(\vec{r}) - w_A(\vec{r})\phi_A(\vec{r}) - w_B(\vec{r})\phi_B(\vec{r}) - p(\vec{r})\left[1-\phi_A(\vec{r})-\phi_B(\vec{r})\right]\right) - \ln Q\left[w_A, w_B\right], \tag{S1}$$

where $\phi_\alpha(r)$ is the volume fraction of species α at position r. $Q[w_A,w_B]$is the partition function of a non-interacting polymer in external fields w_α. The polymer is assumed to be incompressible, so the constraint $\phi_A+\phi_B=1$ is enforced through a pressure field p. The free energy F is compared to the thermal energy k_BT.

The single chain partition function can be evaluated as follows

$$Q = \frac{1}{V}\int drq(\vec{r},1) \tag{S2}$$

where $q(r,s)$ is a restricted chain partition function (propagator) that could be calculated by solving a modified diffusion equation

$$\frac{\partial q}{\partial s} = \begin{cases} \nabla^2 q(\vec{r},s) - w_A(\vec{r})q(\vec{r},s), & 0 \le s < f \\ \nabla^2 q(\vec{r},s) - w_B(\vec{r})q(\vec{r},s), & f \le s < 1 \end{cases}, \tag{S3}$$

subjected to the initial condition $q(r,0)=1$. Since the two ends of the polymer are distinct, a complementary partition function $q^*(r,s)$ is defined similarly and satisfies a similar modified diffusion equation with an initial condition $q(r,1)=1$. Here, we utilize s as a chain contour variable in units of N. All lengths are expressed in units of the unperturbed radius-of-gyration of a polymer, $R_g = (Nb^2/6)^{1/2}$, where b is the statistical segment length. The solution to the modified diffusion equation is conducted following the pseudo-spectral method[1]. An iterative relaxation of the fields towards their saddle-point values is implemented following[2].

By evaluating $q(r,s)$ and its complementary, the segments volume fractions can be determined as follows

$$\phi_A(\vec{r}) = \frac{1}{Q}\int_0^f dsq(\vec{r},s)q^*(\vec{r},s)$$
$$\phi_B(\vec{r}) = \frac{1}{Q}\int_f^1 dsq(\vec{r},s)q^*(\vec{r},s) \tag{S4}$$

The numerical implementation of the SCFT for the entire template is performed on a 2D grid of size $N_x \times N_y = 912 \times 880$ with $L_x \times L_y = 82.08 \times 71.08\ R^2_g$ for ‹11› and $L_x \times L_y = 95.21 \times 82.45\ R^2_g$ for ‹20›, with

periodic boundary conditions in both directions. The volume fraction f and degree of incompatibility χN are chosen such that circular domains (projection of standing cylinders or spheres in 2D) of the minority polymer A are generated. Hence, for the purpose of this work, we chose $f = 0.3$ and $\chi N = 17$.

The role of the directed self-assembly of the polymer domains is depicted through a masking method. A pressure potential $w_+ = (w_B + w_A)/2$ is imposed as a mask on the positions of the post to create excluded areas for the polymer. A magnitude of $w_+ = 10$ is applied for a post size of 7×7 square pixels. To incorporate the effect of surface preferentiality towards minority block in experiments, an exchange potential $w_- = (w_B - w_A)/2 = 30$ is applied surrounding the posts with a thickness of four pixel.

The commensurability of the template pattern is controlled by the ratio of the inter-post distance L_{post} and the polymer equilibrium spacing L_0, which L_p/L_0 = 1.732, and 2.0 are studied in this work. The two commensurate pattern distances 1.732 and 2.0 refer to the special configurations ‹11› and ‹20›, respectively[3]. Furthermore, a spatial Gaussian noise is implemented to slightly shift the positions of the pattern away from the perfect ones. The Gaussian noise is controlled by a parameter ξ, which measures the offset from the equilibrium position, while the direction of the offset can take a random value over the range $[0,2\pi]$, as was discussed in the experimental section.

Figure S9 (a,b) shows an equilibrium distribution of the minority polymer A where long range order is achieved through the application of a commensurate post pattern for the ‹11› and ‹20›, respectively. By just changing the spacing between the post the polymer hexagonal domains rotate by 30°.

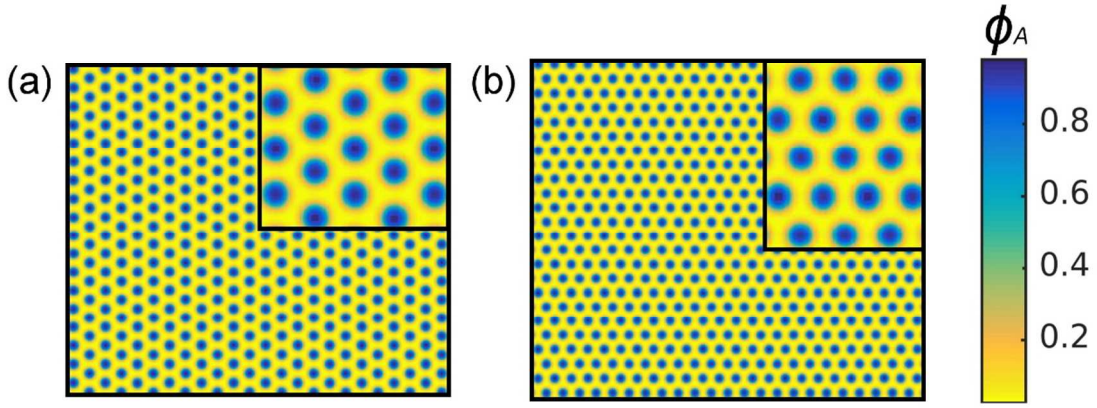

Fig. S9. **Long range order achieved by the application of a noise free commensurate post pattern. (a) Phase ‹11›With L_p/L_0 = 1.732. (b) Phase ‹20›with L_p/L_0 = 2.0.**

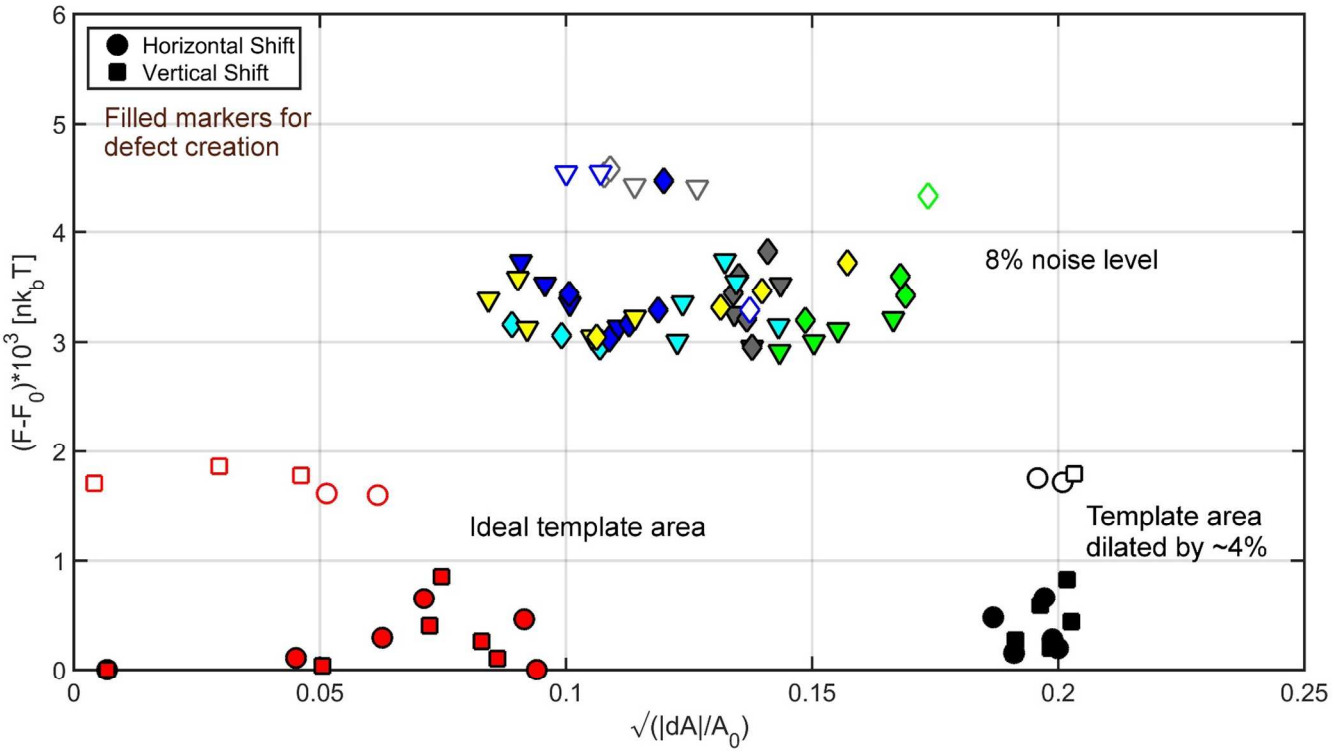

Fig.S10. **Free energy calculations as a function of the distortion parameter $D = \sqrt{(|\Delta A|/A_0)}$ where the markers are identical to figure 4c. The free energy calculations do not show a clear correlation with *D*.**

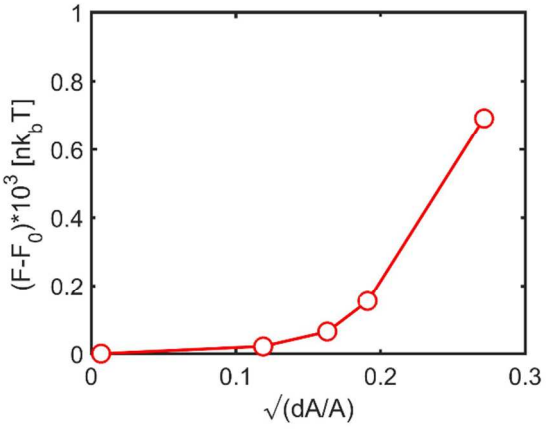

Fig.S11. **The variation of free energy with $D = \sqrt{(|\Delta A|/A_0)}$ of an ideal hexagonal post pattern subjected to pure dilation. The post uniform dilation has a minimal effect on the strain energy below *D = 0.2* after which a pronounced change in slope is observed.**

References

1. Tzeremes, G.; Rasmussen, K.; Lookman, T.; Saxena, A. *Physical Review E* **2002,** 65, (4), 041806.
2. Sides, S. W.; Fredrickson, G. H. *Polymer* **2003,** 44, (19), 5859-5866.
3. Bita, I.; Yang, J. K.; Jung, Y. S.; Ross, C. A.; Thomas, E. L.; Berggren, K. K. *Science* **2008,** 321, (5891), 939-943.